

Ekman Pumping and Storm Energetics

The relationship of Ekman pumping to the vertical phase tilt and energization of the Southern Hemisphere storm track in the context of the Lorenz energy cycle

Cory F. Baggett and Suyoung Lee

Department of Meteorology, The Pennsylvania State University, University Park, Pennsylvania, USA

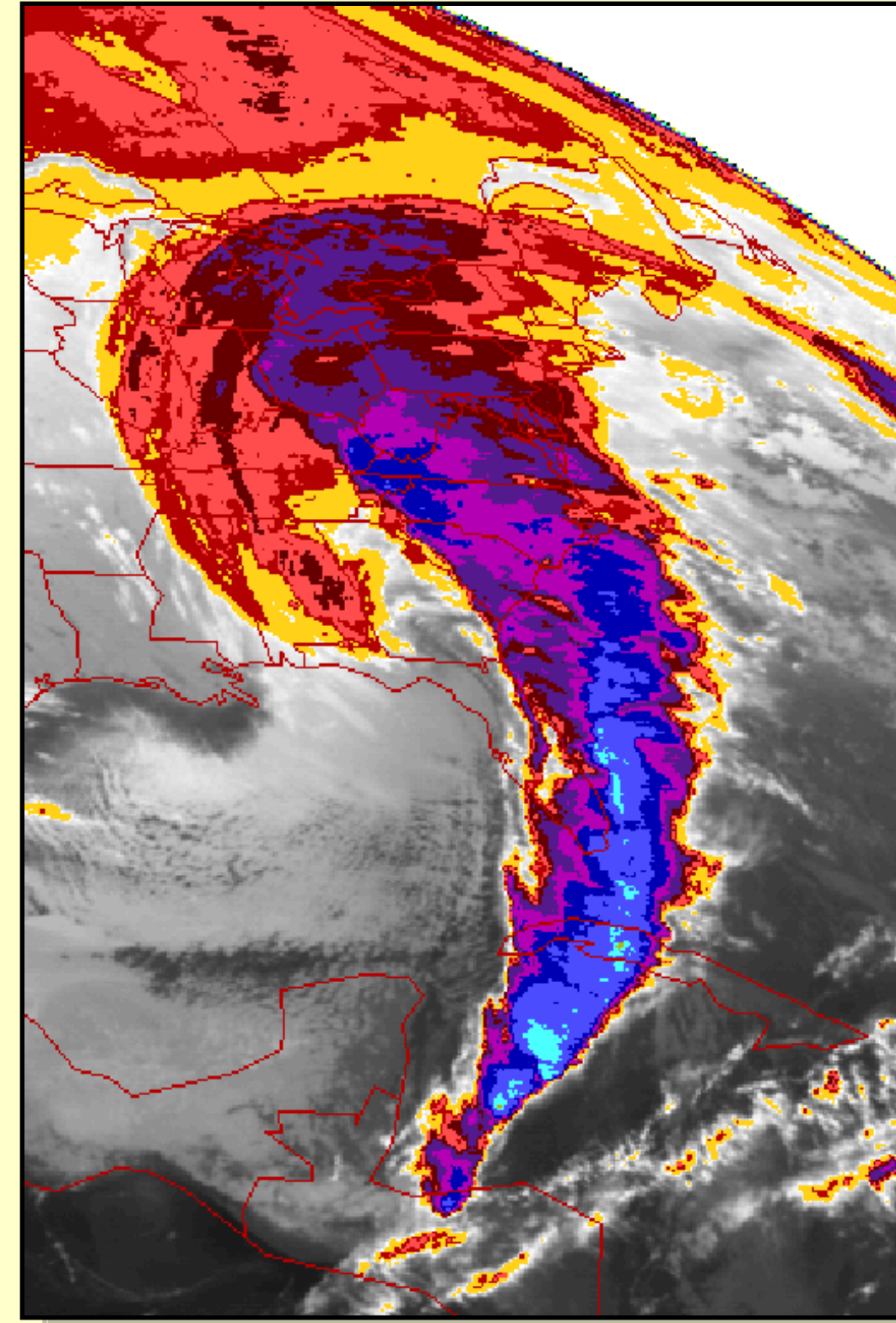
1. Introduction

Atmospheric eddies play a crucial role in the redistribution of earth's energy and moisture. In the mid-latitudes, eddies are the primary drivers of sensible weather in the form of synoptic-scale storm systems.

One mechanism that affects eddies is surface friction. The direct effect of surface friction is to dampen eddy energy. However, in a counter-intuitive fashion, surface friction may indirectly cause storms to grow through a process of dissipative energization induced by Ekman pumping, or it may result in weak horizontal shears that reduce the barotropic decay of the storms.

2. Questions

- (A) What are the climatological values of the Ekman generation of eddy available potential energy (EEPE) and its placement in the storm lifecycle?
- (B) Are positive values of EEPE in the Southern Hemisphere (SH) associated with a small vertical phase tilt, as in Lee (2010b)?
- (C) Does EEPE dissipatively energize the storm track in the SH through the enhancement of baroclinic conversion (Lee 2010b) or through muted barotropic decay (Lee and Held 1991, Lachmy and Harnik 2009, Lee 2010a)?



Superstorm of '93

3. Data, Methods, and Notation

- Daily ERA-Interim reanalysis (1979-2011), 2.5° by 2.5°, 23 vertical levels
- Perform the study in the context of the Lorenz energy cycle (Lorenz 1955)
- Energetics are calculated according to Peixoto and Oort (1974)
- Employ spectral analysis to determine the vertical phase tilt of the SH
- Apply composite analysis to determine the association of EEPE to the SH vertical phase tilt and to the SH storm lifecycle
- Use one-point correlation maps of v-wind to examine eddy structure

Notation	Description	Notation	Description
K_E	Eddy kinetic energy	K_{E+}	Days when $K_E > 1\sigma$
K_M	Zonal kinetic energy	$EEPE+ K_{E+}$	Days when $K_E > 1\sigma$ on lag 0 and $EEPE > 1\sigma$ on lag +2
P_E	Eddy available potential energy	$EEPE- K_{E+}$	Days when $K_E > 1\sigma$ on lag 0 and $EEPE < 0$ on lag +2
P_M	Zonal available potential energy		
$C(X, Y)$	Energy conversion rate (from X to Y)		
$C(P_E, K_E)$	Eddy conversion		
$C(P_M, P_E)$	Baroclinic conversion		
$C(K_E, K_M)$	Barotropic decay		

4. Definition of EEPE

Calculate Ekman pumping vertical velocity at the top of the boundary layer:

$$w_{Ek} = \frac{1}{f\rho} \left(\frac{\partial \tau_y}{\partial x} - \frac{\partial \tau_x}{\partial y} \right) \Rightarrow \omega_{Ek} = -\bar{\rho} g w_{Ek}$$

Assume uniform horizontal divergence between the top of the boundary layer and the tropopause:

$$\omega_{Ek}|_p = \omega_{Ek}|_{p_{BL}} \left(\frac{p - p_T}{p_{BL} - p_T} \right)$$

Substitute into Lorenzian energetics:

$$EEPE = C_{Ek}(K_E, P_E) = R_d \int p^{-1} \omega_{Ek} \overline{T'dm}$$

Cold air rising or warm air sinking corresponds to $EEPE > 0$.

Ekman generation of Eddy available Potential Energy

5. Climatological Values of EEPE

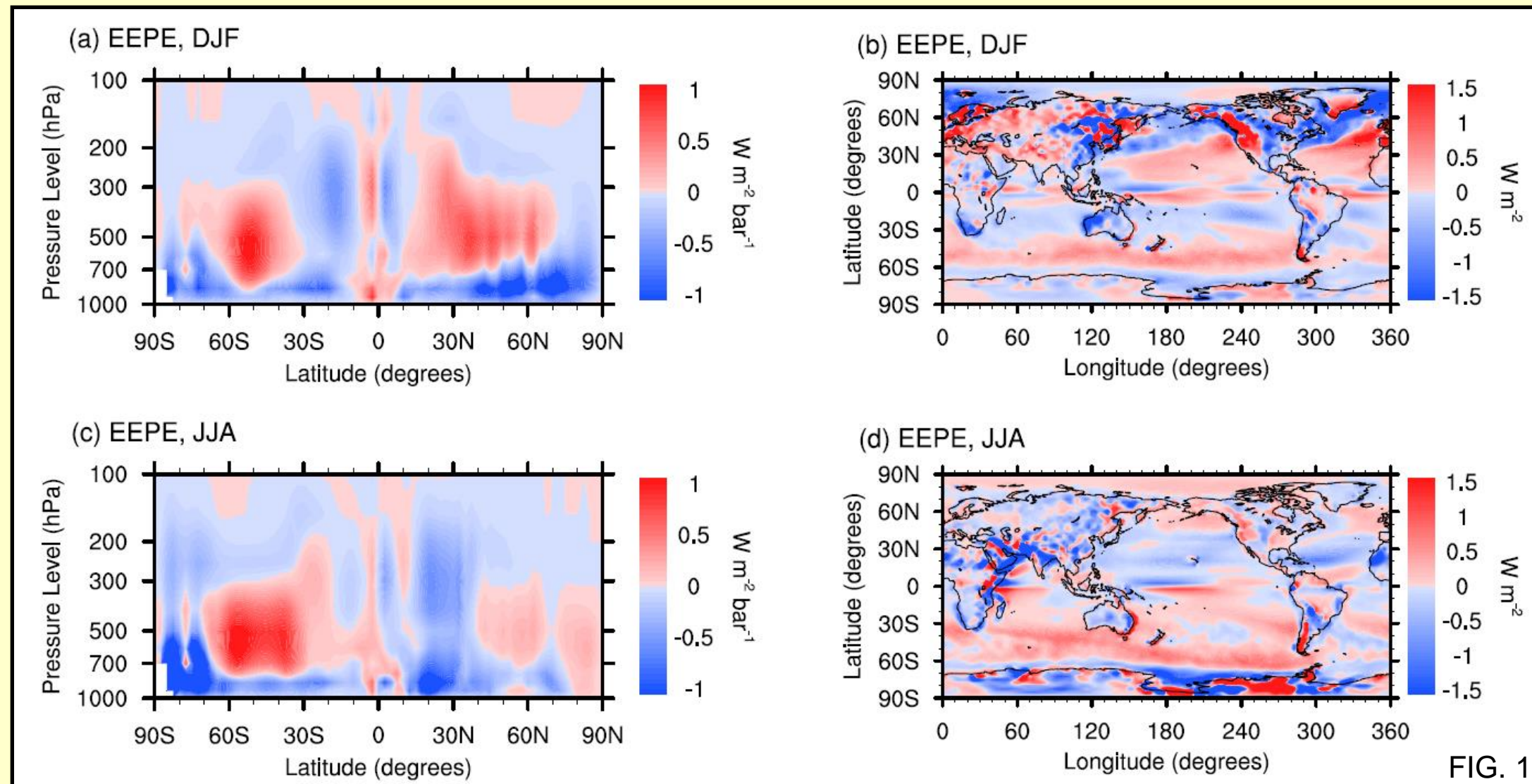


FIG. 1

- Integrating EEPE yields a positive (negative) value in the SH (NH)
- EEPE peaks during a given hemisphere's winter
- EEPE is positive in the mid-troposphere near the climatological positions of the jets
- EEPE is predominantly negative in the lower troposphere

6. EEPE versus SH Vertical Phase Tilt

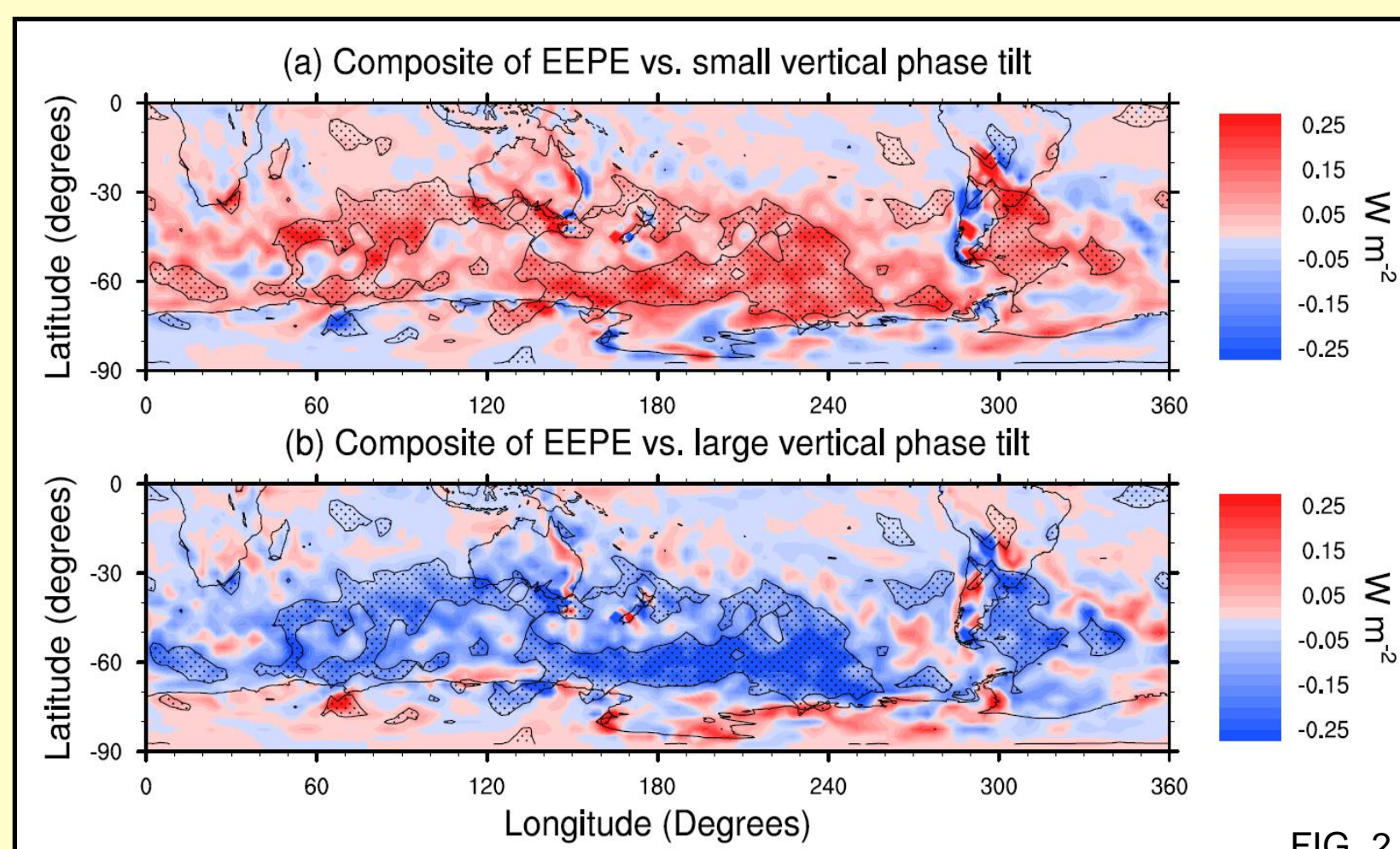


FIG. 2

Small vertical phase tilt is associated with positive EEPE

Large vertical phase tilt is associated with negative EEPE

7. SH Winter Storm Lifecycle Composites

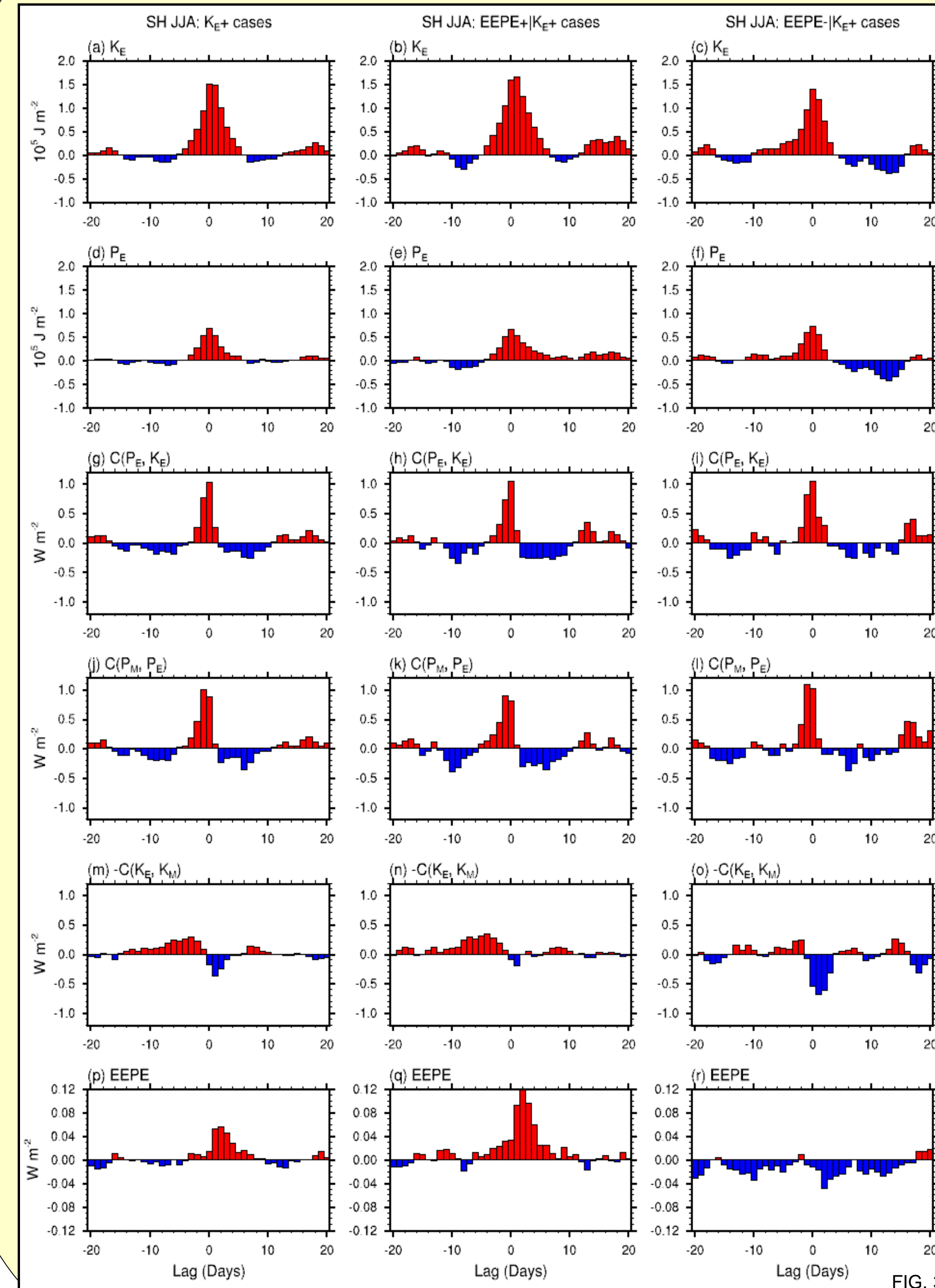


FIG. 3

Enhancement of K_E for positive EEPE

Persistently positive P_E for positive EEPE

No significant differences in eddy conversion

No significant differences in baroclinic conversion

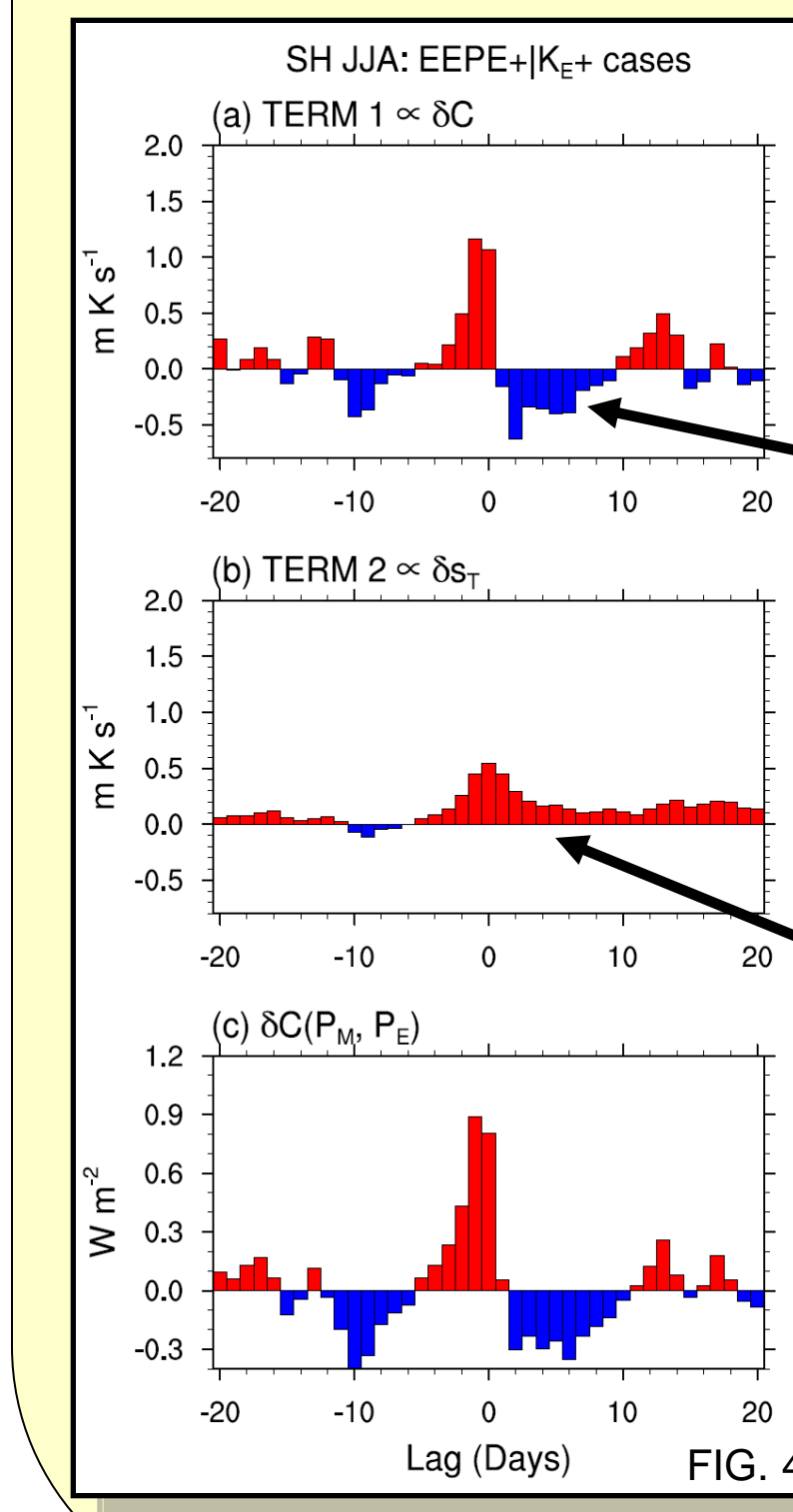
Weak barotropic decay for positive EEPE

EEPE peaks on lag +2 in the storm lifecycle

8. Baroclinic Conversion

$$\delta C(P_M, P_E) \propto \delta(\overline{v'T'})$$

$$\delta(\overline{v'T'}) \cong s_v(s_T)_{CLIM} \delta C + s_v C_{CLIM} \delta s_T$$



Positive EEPE is associated with a small vertical phase tilt which reduces the correlation between v and T. This reduction in correlation dominates over the enhancement of the standard deviation of eddy T. Therefore, positive EEPE does not exhibit an enhancement of baroclinic conversion.

FIG. 4

9. Barotropic Decay

$$-\frac{\partial \overline{u'v'}}{\partial y} > 0 \Rightarrow \frac{\partial \overline{u}}{\partial t} > 0 \Rightarrow K_M \uparrow$$

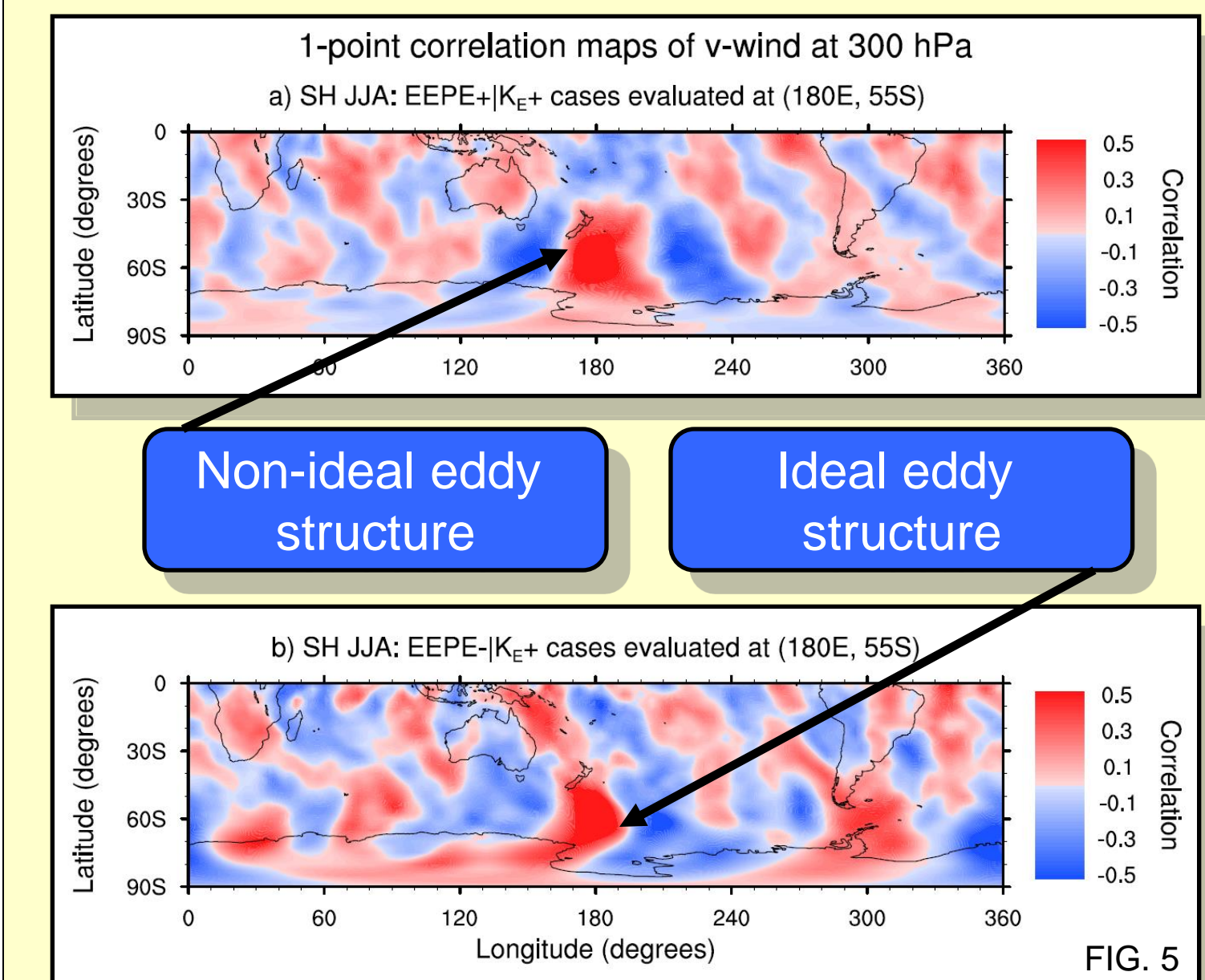


FIG. 5

Non-ideal eddy structure

Ideal eddy structure

Eddy structure of positive EEPE is not conducive to eddy momentum flux convergence. Therefore, positive EEPE exhibits muted barotropic decay.

10. Results and Future Work

The Ekman generation of eddy available potential energy energizes the storm track through its association with muted barotropic decay rather than enhanced baroclinic conversion.

Additional investigation should include an analysis of the cause for this association, the Northern Hemisphere, and individual storm case studies. Furthermore, because eddies are the primary drivers of climate in the mid-latitudes, long-term variability of EEPE should be explored in the context of a changing climate. In doing so, the relationship of EEPE to tropical convection should be explored.

Figure Captions

FIG. 1. 1979-2011 climatological means of the Ekman generation of eddy available potential energy (EEPE). Positive (negative) values indicate the conversion of K_E to P_E (P_E to K_E) as a result of Ekman pumping.
 FIG. 2. SH anomaly composites of EEPE on days when the anomalous phase difference between the upper (300 hPa) and lower (925 hPa) levels of the atmosphere between 30°S and 70°S is (a) less than negative one standard deviation and (b) greater than one standard deviation. The contoured stippled regions indicate areas of 95% confidence in the difference between the two composites evaluated with a t-test.
 FIG. 3. SH lag anomaly composites during JJA of the energetics and EEPE where the first column is composited against K_E anomalies greater than one standard deviation on lag 0 such that only the days with the greatest K_E in a 7 day time period are selected. The second column is the same as the first with the additional condition that EEPE anomalies are greater than one standard deviation on lag +2. The third column is the same as the first with the additional condition that EEPE anomalies are negative on lag +2.
 FIG. 4. As in column 2 of Fig. 3 except the values being composited are a) $-s_v(s_T)_{CLIM} \delta C$, b) $-s_v C_{CLIM} \delta s_T$, and c) $\delta C(P_M, P_E)$.
 FIG. 5. One-point correlation maps conducted at (180E, 55S) of v-wind for the SH during JJA for a) the days used in column 2 of Fig. 3 and b) the days used in column 3 of Fig. 3.

Key References

Lachmy, O., and N. Harnik, 2009: A Wave Amplitude Transition in a Quasi-Linear Model with Radiative Forcing and Surface Drag. *J. Atmos. Sci.*, **66**, 3479-3490.
 Lee, S., 2010: Finite-amplitude equilibration of baroclinic waves on a jet. *J. Atmos. Sci.*, **67**, 434-451.
 Lee, S., 2010: Dissipative energization of baroclinic waves by surface Ekman pumping. *J. Atmos. Sci.*, **67**, 2251-2259.
 Lee, S., and I. M. Held, 1991: Subcritical Instability and Hysteresis in a Two-Layer Model. *J. Atmos. Sci.*, **48**, 1071-1077.
 Lorenz, E. N., 1955: Available potential energy and the maintenance of the general circulation. *Tellus*, **7**, 157-167.
 Peixoto, J. P., and A. H. Oort, 1974: The annual distribution of atmospheric energy on a planetary scale. *J. Geophys. Res.*, **79**, 2149-2159.
Acknowledgments
 This study was supported by the National Science Foundation under Grant ATM-1139970. Valuable comments were provided by Steven Feldstein and Michael Goss. All coding was performed using the National Center for Atmospheric Research Command Language.